84-1112
cy001

TM NO. 841112

841112   001N

NAVAL UNDERWATER SYSTEMS CENTER
NEW LONDON LABORATORY
NEW LONDON, CT 06320

TECHNICAL MEMORANDUM

Scattering From Gratings of High Aspect Ratio Compliant Tubes
Embedded in an Elastomer Layer

Date: 21 June 1984   Prepared by: *Ronald P. Radlinski*
                                       RONALD P. RADLINSKI

                                       Robert S. Janus
                                       ROBERT S. JANUS

                               -. SURFACE SHIP SONAR DEPARTMENT
                        MECH ENGRG & ACOUSTICS APPLIC. DIVISION

Report Documentation Page

Public reporting burden for the collection of information is estimated to average 1 hour per response, including the time for reviewing instructions, searching existing data sources, gathering and maintaining the data needed, and completing and reviewing the collection of information. Send comments regarding this burden estimate or any other aspect of this collection of information, including suggestions for reducing this burden, to Washington Headquarters Services, Directorate for Information Operations and Reports, 1215 Jefferson Davis Highway, Suite 1204, Arlington VA 22202-4302. Respondents should be aware that notwithstanding any other provision of law, no person shall be subject to a penalty for failing to comply with a collection of information if it does not display a currently valid OMB control number.

1. REPORT DATE **21 JUN 1984**	2. REPORT TYPE **Technical Memo**	3. DATES COVERED **21-06-1984 to 21-06-1984**

4. TITLE AND SUBTITLE **Scattering from Gratings of High Aspect Ratio Compliant Tubes Embedded in an Elastomer Layer This paper was presented to the 106th meeting of the Acoustical Society of America, held in San Diego, CA during November of 1983**	5a. CONTRACT NUMBER
	5b. GRANT NUMBER
	5c. PROGRAM ELEMENT NUMBER
6. AUTHOR(S) **Ronald Radlinski; Robert Janus**	5d. PROJECT NUMBER **A70204 and ZN00001**
	5e. TASK NUMBER
	5f. WORK UNIT NUMBER
7. PERFORMING ORGANIZATION NAME(S) AND ADDRESS(ES) **Naval Underwater Systems Center,New London,CT,06320**	8. PERFORMING ORGANIZATION REPORT NUMBER **TM 841112**
9. SPONSORING/MONITORING AGENCY NAME(S) AND ADDRESS(ES)	10. SPONSOR/MONITOR'S ACRONYM(S)
	11. SPONSOR/MONITOR'S REPORT NUMBER(S)

12. DISTRIBUTION/AVAILABILITY STATEMENT **Approved for public release; distribution unlimited**

13. SUPPLEMENTARY NOTES **NUWC2015**

14. ABSTRACT
An analytical formulation is presented for normal incident plane wave scattering from gratings of compliant tubes embedded in a viscoelastic layer immersed in fluid. Approximations to boundary conditions at the interfaces between the interstice and compliant elements 1 are modified by treating the interstice as a viscoelastic plate which has the material properties of the polymer matrix material. The compliant tubes are modeled as two structurally and acoustically coupled plates with end conditions which correspond to those for the vibrational modes of a highly eccentric long cylindrical shell. Conditions on normal displacement, normal stress, and tangential displacement relate the compliant plates and viscoelastic plate boundaries to the surrounding viscoelastic layers. Comparisons of the insertion loss for gratings in fluid and gratings in viscoelastic layers in fluid are shown. Limitations of the analysis are discussed and calculations will be compared with experimental data.

15. SUBJECT TERMS
Multiple scattering from shells; boundary layers

16. SECURITY CLASSIFICATION OF:			17. LIMITATION OF ABSTRACT	18. NUMBER OF PAGES	19a. NAME OF RESPONSIBLE PERSON
a. REPORT **unclassified**	b. ABSTRACT **unclassified**	c. THIS PAGE **unclassified**	**Same as Report (SAR)**	**25**	

NAVAL UNDERWATER SYSTEMS CENTER
NEW LONDON LABORATORY
NEW LONDON, CT 06320

TECHNICAL MEMORANDUM

Scattering From Gratings of High Aspect Ratio Compliant Tubes
Embedded in an Elastomer Layer

Date: 21 June 1984   Prepared by: *Ronald P. Radlinski*
                                          RONALD P. RADLINSKI

                                          Robert S. Janus
                                          ROBERT S. JANUS

                            SURFACE SHIP SONAR DEPARTMENT
                        MECH ENGRG & ACOUSTICS APPLIC. DIVISION

ABSTRACT

An analytical formulation is presented for normal incident plane wave scattering from gratings of compliant tubes embedded in a viscoelastic layer immersed in fluid. Approximations to boundary conditions at the interfaces between the interstice and compliant elements[1] are modified by treating the interstice as a viscoelastic plate which has the material properties of the polymer matrix material. The compliant tubes are modeled as two structurally and acoustically coupled plates with end conditions which correspond to those for the vibrational modes of a highly eccentric long cylindrical shell. Conditions on normal displacement, normal stress, and tangential displacement relate the compliant plates and viscoelastic plate boundaries to the surrounding viscoelastic layers. Comparisons of the insertion loss for gratings in fluid and gratings in viscoelastic layers in fluid are shown. Limitations of the analysis are discussed and calculations will be compared with experimental data.

This paper was presented to the 106th meeting of the Acoustical Society of America, held in San Diego, CA. during November of 1983.

ADMINISTRATIVE INFORMATION

I.   Introduction

In previous presentations, the interaction between multiple gratings of compliant tubes in fluid has been discussed for several different grating configurations. In this work, the transmission of plane waves through a single grating of the compliant tubes embedded in a finite thickness viscoelastic material, surrounded by fluid, will be investigated through extensions of the fluid model. Plane strain viscoelastic theory is used to describe the elastomeric layer. The structural modes of the compliant tubes are treated as two coupled plates with vibrations corresponding to those of an highly eccentric oval shell. Differences between modeling the interstice between the tubes as an elastic layer or a thin elastic plate are shown to be material dependent. In both cases, the layer thickness transmissions resonances resulting from shear wave generation by the compliant tube inclusions are found to be significant in elastic layers. The introduction of damping into the elastomer mitigates the transmission peaks due to the thickness resonances. Comparisons of theoretical calculations with experimental measurements of insertion loss for panels with low and medium stiffness viscoelastic material are found to be in reasonable agreement.

II. THEORY

A schematic representation of the compliant tube grating embedded in a viscoelastic layer is shown in figure 1. A normally incident plane wave that transverses region 1 strikes the elastic layer at the boundary of region 2 and a part of this wave is reflected.

The portion of the incident wave which enters the region 2 undergoes multiple reflections, at both the tube and elastic-fluid boundaries and is either absorbed or finally emitted from the layer to either region 1 or region 5. Because of a net

volume displacement generated near the symmetric bending resonance frequencies of the plates, the tubes perform as acoustically soft inclusions. Shear waves are generated even at normal incidence through the bending and rigid body translational motion of the tubes. Because of the symmetry in this grating arrangement, the solution reduces to satisfying the boundary conditions between any two planes of symmetry. Since the solution in the intertices between tubes differs from the rest of the layer, the encapsultant layer is divided into three regions.

The boundary condition in the fluid at the symmetry planes is that the transverse velocity is zero. In the elastomeric material, the additional boundary condition is zero transverse shear at the symmetry planes.

The total pressure in the fluid above the elastomer (region 1 in figure 1) is the sum of the incident plane and an infinite series of reflected waves as given by the first expression in figure 2. R_n represents an unknown scattering coefficient. The wavenumber of the nth reflected wave, namely k_n, is real when k_o, the wavenumber in the fluid, is greater than the grating parameter α_n. In this case the reflected wave propagates away from the grating into the fluid. For k_o less than α_n, k_n is imaginary and an evanescent wave propagates nearly parallel to the grating and decays exponentially away from the grating. In the assumed linear viscoelectic layer, the scalar and vector displacement potentials for the dilatational (ϕ_j) and shear waves (A_j) in the jth elastomer region are given as infinite series of inhomogeneous waves traveling in both directions. The dilatational and shear wavenumbers k_p and k_s respectively are assumed complex. The constant c_j is determined by the region geometry. $A_m^{(j)}$, $B_m^{(j)}$, $C_m^{(j)}$, and $D_m^{(j)}$, are scattering coefficients determined by satisfying the boundary conditions at the region interfaces. Later the interstice (region 3) will be modeled as a viscoelastic thin plate and compared with the interstice modeled as a viscoelastic layer.

4

Implicit in the solutions for the viscoelastic interstice layer between tubes is the assumption that at both the symmetry plane bisecting the interstice between the tubes and at the tube-elastomer abuttment, u_y and σ_{xy} are zero. The assumption that σ_{xy} is zero at the tube abuttment implies that the shearing stress caused by the motion of the symmetric clamped end modes is negligible. If the tubes are thin enough this assumption is reasonable. Because of symmetry, the condition on u_y is explicitly true. The guided end conditions are matched by the assumed solution.

Of particular interest in this presentation is the transmitted pressure in region 5 of figure 1. For grating spacings less than a wavelength in the fluid, the transmitted pressure in the field is determined by T_0, which is the scattering coefficient of the single transmitted propagating wave.

The plates are assumed to obey the thin plate theory. The totally symmetric modes of the compliant tube which result in a net volume displacement are approximated by clamped end conditions, and are shown in part I of figure 3. The asymmetric modes shown in part III include rigid body motion and are described by guided end conditions or zero slope and zero transverse shear. Complete descriptions of these wave functions are described in references 2 and 3.

When the interstice is modeled as a viscoelastic plate, the boundary conditions are chosen to match those for the tube model shapes. However, as seen in part II of figure 3, the motion of the viscoelastic plate is different than for the two connected plates in the sense that the motion is asymmetric with respect to the major axis of the plate. The guided end conditions result in identical mode shapes of the two coupled plates of the tube and the interstice modeled as a thin viscoelastic plate. The limitation of modeling the interstice as a thin viscoelastic

plate is the small range of viscoelastic materials for which the thin plate theory is valid. From Junger and Feit[4], the frequency range that the classical thin plate theory is adequate is restricted to:

$$\frac{h}{\pi c_s} < 0.1 \qquad\qquad (1)$$

Here c_s is the shear wave speed of the material and h is the interstice thickness. For frequencies larger than the above restriction, rotational inertia and transverse shear must be included. At even higher frequencies, compressional wave effects must also be included in the modeling of the intertice. Damping effects have been incorporated into the plate theory by assuming a complex Young's modulus.

The mathematical expressions for the wave functions which describe clamped and guided end conditions are shown in figure 4. Both expressions contain even terms because only modes symmetric with respect to the center (x-axis) of the tube are excited by the normally incident plane wave. The resonance frequency is proportional to the square of the wavenumber. The first non-zero, in-air frequency of the guided modes occurs approximately 1.8 times the value for the first totally symmetric compliant mode. The non-zero frequency, guided end modes have been shown to degrade insertion loss performance for closely space multiple gratings[2].

The boundary conditions to be satisfied at the various region interfaces are displayed in figure 5. The fluid-elastomer and elastic-elastic conditions are those common for plain strain problems. The continuity of tangential displacement at the plate-elastometer boundary is derived by assuming inextentional motion of the plate such that

$$V_{tan} = \frac{h}{2} \frac{dW}{dy} \qquad\qquad (2)$$

III. NUMERICAL EXAMPLES

In the first example, the encapsulant is treated as a elastic material with zero damping for two values of the shear modulus. The dilatational modulus and density of the elastic material is similar to that of water. The insertion loss defined as $20 \log_{10}(P_i/P_t)$ is a measure of the energy transmitted through the baffle. A large insertion loss implies that the transmitted energy is small. The frequency axis has been normalized to f_1 which is the first symmetric flexural resonance of a single tube in air. The same normalization will be used throughout the remainder of the paper. The thickness of the interstice layer is about $0.013 \lambda_1$ where λ_1 is the acoustic wavelength at f_1. The elastic separation between the tubes is about the one tube width. Using the equation (1) for the validity of the thin plate theory that indicates that for the higher shear modulus (10^9 nt/m^2) the classical plate theory should be a good approximation to $3f_1$.

As seen in the right hand side of the figure 6, good agreement is found between plate theory and elastic layer calculations. Although not shown, the agreement is consistent down to $0.25f_1$. For the low shear modulus material (10^6nt/m^2) classical plate theory is valid only below $0.25f_1$ and poor agreement is found between the interstice (region 3) modeled as a plate versus the intertice modeled as an elastic layer with approximated boundary conditions at the tube elastomer abutment. The conclusion is that only for very stiff elastomers will the plate model be valid for tubes with significant separation distances d. Studies with closely packed arrays indicated the modeling of the interstice in these cases is not sensitive in the sense that the viscoelastic separation acts simply as a mass.

In the second example showed in figure 7, the effects of the encapsulant as a function of shear modulus are shown for densely packed compliant tubes. The insertion loss for an identical unencapsulated grating is shown by the solid curve.

The layer model is used for the interstice but as mentioned above, the interstice is insensitive to the two modeling techniques for densely packed tubes. The maxima in the insertion loss at about $1.2f_1$ and $6.0f_1$ are due to the first two totally symmetric clamped tube modes. The exact location of the maxima are determined by array fluid interactions. When the tubes are encapsulated in the low stiffness elastomer, the location of the maxima do not change but the depth of the null decreases. Part of this depth of the null difference is due to the damping factor ($\delta = 0.2$). As the stiffness is increased to $\mu = 10^8$ nt/m and the damping factor increases to 0.5, the character of the insertion loss changes dramatically. The additional stiffness on the tube increases the effective resonance frequency of the structural modes. The stiffness also decreases the vibrational motion of the layer so that more energy tends to be transmitted through the layer.

The effects of damping are shown in figure 8. In this example, an elastic layer is compared with the stiffer viscoelastic layer of figure 7. The large oscillations in the insertion loss are due to thickness resonances of the elastic layer from the resulting shear waves generated by the motion of the tube. The damping in the viscoelastic material converts these shear waves to heat and thus smooth the response of the insertion loss curves.

The effects of the thickness of the elastomer are shown in figure 9 for two thicknesses. The thickness of the original layer (t_0) is $\lambda_1/8$ or $0.56\lambda_s$ where λ_s is the shear wavelength at f_1. When the thickness of the encapulating layer is reduced, two effects control the changes in the insertion loss. First, the decreased thickness of the elastomer reduces the effective stiffness surrounding the tube walls. Second, thinning the layer will shift the layer thickness resonances to higher frequencies. In figure 9, it appears that the decreased stiffness is the dominate effect which not only lowers the insertion loss maximum

8

of the first symmetric mode to $1.5f_1$ but also allows a higher amplitude of vibration such that more energy is reflected at the resonance maxima.

IV. COMPARISON OF THEORY AND MEASUREMENTS

In the last two figures, the calculations for the insertion loss for two encapsulants with tubes densely packed are compared with experimental data. The interstice is modeled as a viscoelastic layer. The first comparison is shown in figure 10 for the encapsulant with the low shear modulus material. Differences between experimental and the theoretical calculations can be attributed to the nominal values of the shear values used for the calculation. The material measurements made with the B&K Young's modulus apparatus as discussed in reference 5 have large uncertainties for low shear materials. The castable B.F. Goodrich ρc rubber material is relatively temperature insensitive.

The second comparison between calculations and theory is shown in figure 11 for a closely packed tube grating encapsulated in the high shear modulus polyurethane. Again reasonable agreement is found over the entire frequency spectrum.

V. CONCLUSIONS

The parameters which affect the transmissivity of energy through an encapsulated compliant tube grating include the dynamic compliance of the compliant tubes, the stiffness and damping factor of the encapsulant material, and the thickness of the layer. Low stiffness materials with some damping to smooth the thickness resonances do not significantly alter the unencapsulated grating performance. Higher stiffness materials increase the frequency of highest dynamic insertion loss but also decrease the dynamic compliance. The layer thickness resonances are most pronounced in purely elastic materials. For a given

thickness, the layer resonances were more prominent in stiffer viscoelastic materials in which the longer wavelengths make absorption of shear waves more difficult.
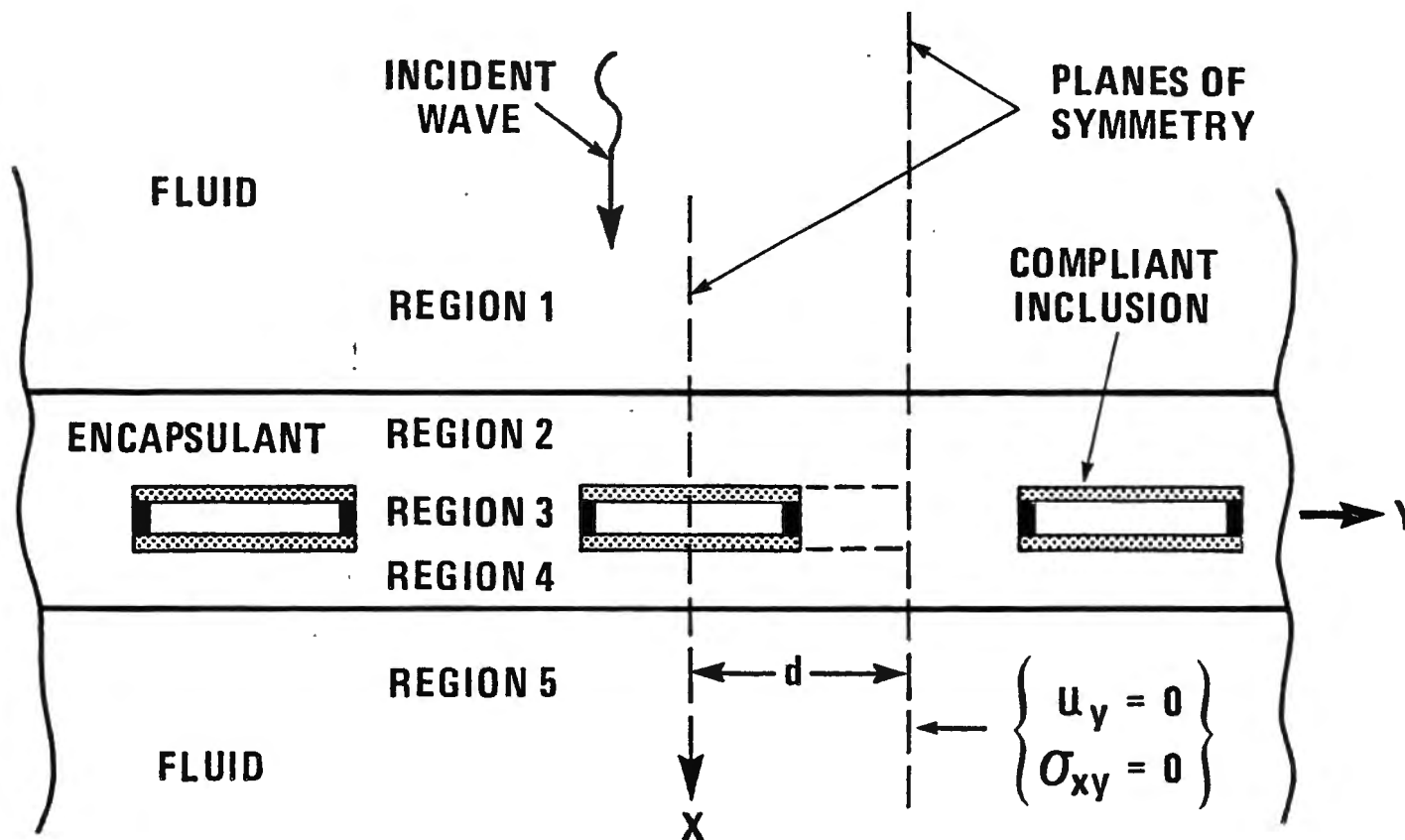
In the frequency range where the classical thin plate theory is valid, good agreement occurs between layer and plate modeling of the interstice. For closely space gratings, modeling of the interstice is not sensitive to either the plate or viscoelastic layer model. However, it is noted that modeling the interstice as a fluid but retaining region 2 and region 4 as viscoelastic layers gave significantly different results than the two interstice models discussed in this presentation.

VI. REFERENCES

1. R. P. Radlinski, "Scattering of Plane Waves From A Compliant Tube Grating in a Linear Viscoelastic Layer" NUSC TR 5433, 18 August 1977.

2. R. P. Radlinski and M. M. Simon, "Scattering by multiple gratings of compliant tubes," J. Acoust. Soc. Am. 72(2), August, 1982 pp. 607-614.

3. R. P. Radlinski and M. M. Simon, "Erratum: Scattering by multiple gratings of compliant tubes," J. Acoust. Soc. Am. 74(5), Nov, 1983 p. 1646.

4. M.C. Junger and D. Feit, Sound, Structures and Their Interactions, MIT Press, Cambridge, MA, 1972.

5. R. E. Strakna, "Determination of the Complex Young's Modulus of Selected Polymers Using the WLF Transformation," NUSC Tech. Report 5251, 16 Oct. 1975

ENCAPSULATED COMPLIANT TUBE GRATING

INCIDENT WAVE

PLANES OF SYMMETRY

FLUID

REGION 1

COMPLIANT INCLUSION

ENCAPSULANT   REGION 2

REGION 3

REGION 4

$\rightarrow$ Y

REGION 5

d

$\left\{ \begin{array}{c} u_y = 0 \\ \sigma_{xy} = 0 \end{array} \right\}$

FLUID

X

L3818bS

FIGURE 1

INCIDENT AND REFLECTED PRESSURE WAVES

$$P_1 = e^{ik_o x} + \sum_{n=o}^{\infty} R_n e^{-ik_n x} \cos \alpha_n y$$

$$k_n^2 = k_o^2 - \alpha_n^2 ; \quad \alpha_n = \frac{n\pi}{d}$$

DISPLACEMENT POTENTIALS FOR DILATIONAL & SHEAR WAVES

$$\phi_j = \sum_{m=o}^{\infty} \left\{ A_m^{(j)} e^{ik_{m_p} x} + B_m^{(j)} e^{-ik_{m_p} x} \right\} \cos \alpha_m (y - c_j)$$

$$A_j = \sum_{m=o}^{\infty} \left\{ C_m^{(j)} e^{ik_{m_s} x} + D_m^{(j)} e^{-ik_{m_s} x} \right\} \sin \alpha_m (y - c_j)$$

$$k_{m_p}^2 = k_p^2 - \alpha_m^2 ; \quad k_{m_s}^2 = k_s^2 - \alpha_m^2 ; \quad \alpha_m = \frac{m\pi}{d - c_j}$$

$k_p \equiv$ complex dilational wavenumber

$k_s \equiv$ complex shear wavenumber

TRANSMITTED PRESSURE WAVES

$$P_5 = \sum_{n=o}^{\infty} T_n e^{ik_n x} \cos \alpha_N Y$$

FIGURE 2

I. CLAMPED MODES FOR TUBES

FUNDAMENTAL
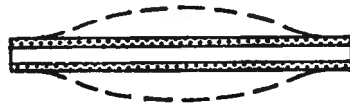
SECOND

II. CLAMPED MODES FOR VISCOELASTIC LAYER

III. ZERO SLOPE AND ZERO TRANSVERSE FORCE MODES FOR TUBES AND VISCOELASTIC LAYER

RIGID BODY

SECOND

L3818aS

FIGURE 3
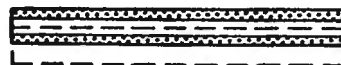
I. CLAMPED END CONDITIONS

$$W(y) = \sum_{s=0}^{\infty} W_s (\cos k_s y + c_s \cos h\, k_s y)$$

$$\omega_s = \frac{h}{\sqrt{12}} k_s^2 c_p$$

$$k_s = \frac{(2s + {}^3/_2)\,\pi}{2b}$$

$$c_p = \sqrt{\frac{E}{\rho(1-\sigma^2)}} \qquad c_s = \frac{\cos k_s b}{\cos h\, k_s b}$$

II. ZERO SLOPE AND ZERO TRANSVERSE FORCE END CONDITIONS

$$W(y) = \sum_{s=0}^{\infty} W_s \cos k_s y$$

$$\omega_A = \frac{h}{\sqrt{12}} k_s^2 c_p$$

$$k_s = \frac{s\,\pi}{b}$$

L3818eS

FIGURE 4

BOUNDARY CONDITIONS

FLUID – ELASTOMER INTERFACES

    (1) ZERO SHEAR STRESS

    (2) NORMAL DISPLACEMENT CONTINUOUS

    (3) NORMAL STRESS EQUAL NEGATIVE PRESSURE IN FLUID

ELASTIC – ELASTIC REGION BOUNDRIES

    (1) NORMAL AND TANGENTIAL DISPLACEMENTS CONTINUOUS

    (2) NORMAL AND TANGENTIAL STRESSES CONTINUOUS

PLATE – ELASTOMER INTERFACE

    (1) NORMAL AND TANGENTIAL DISPLACEMENTS CONTINUOUS

    (2) THIN PLATE EQUATION
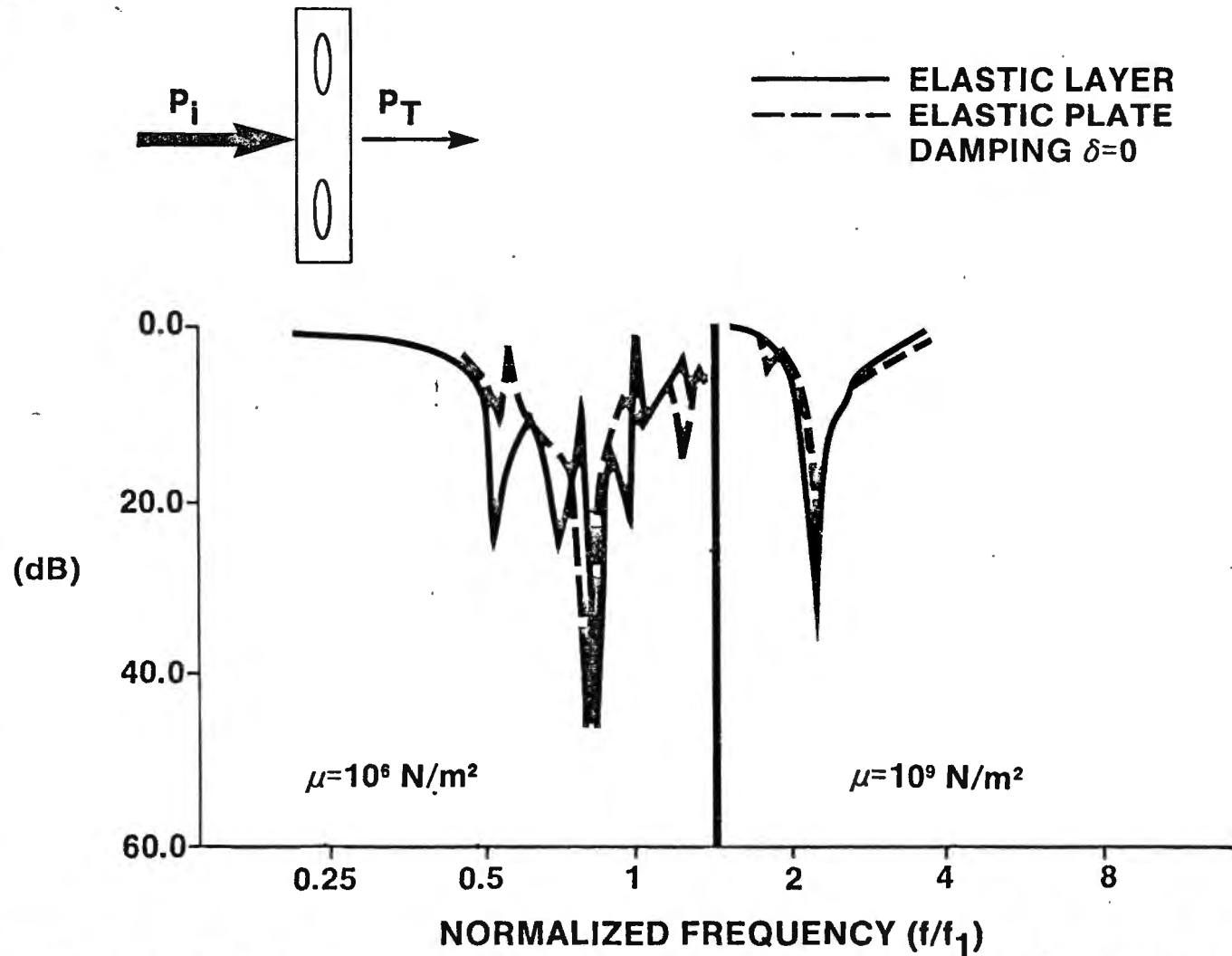
L3818dS

FIGURE 5

CALCULATED INSERTION LOSS (20 log P_i/P_T)

FIGURE 6

L3818fS

CALCULATED INSERTION LOSS (20 log P_i/P_T)
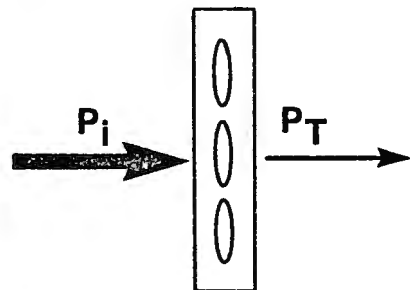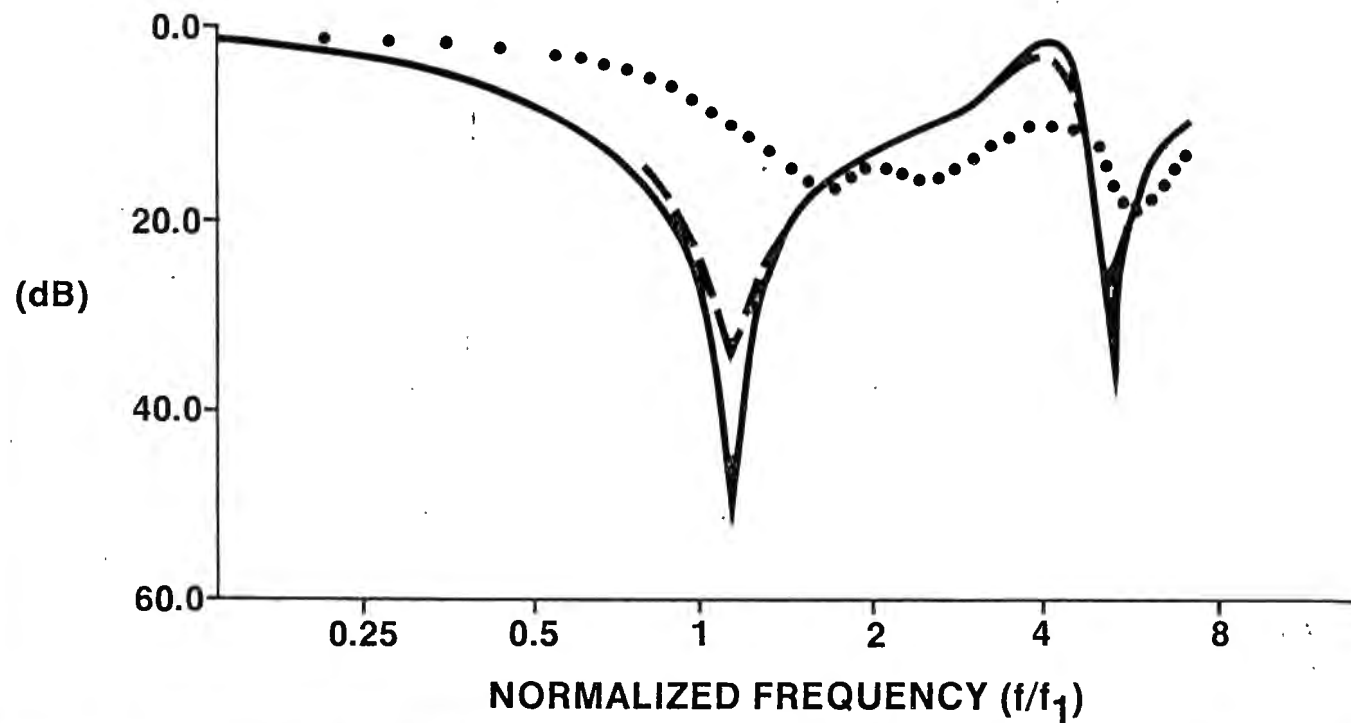
FIGURE 7

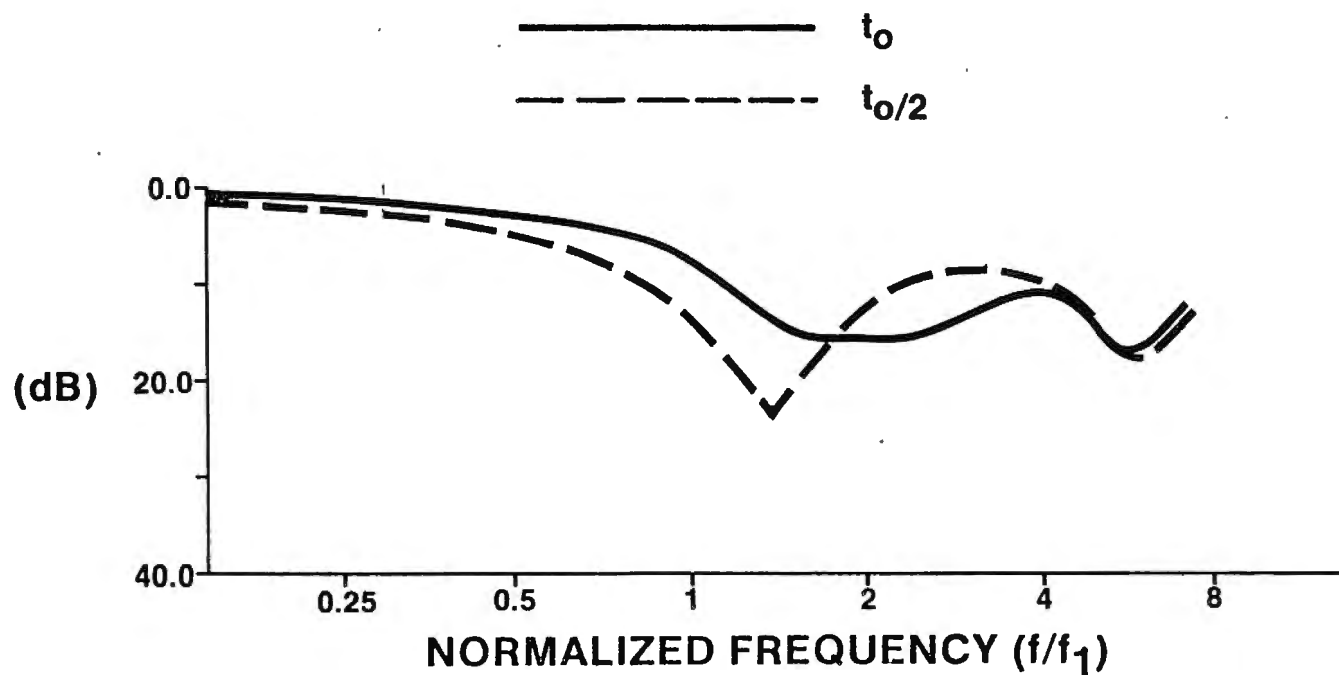# CLACULATIONS OF INSERTION LOSS FOR LOSS FACTOR VARIATIONS IN HIGH SHEAR MODULUS MATERIAL $(\mu = 10^8 \text{ N/m}^2)$
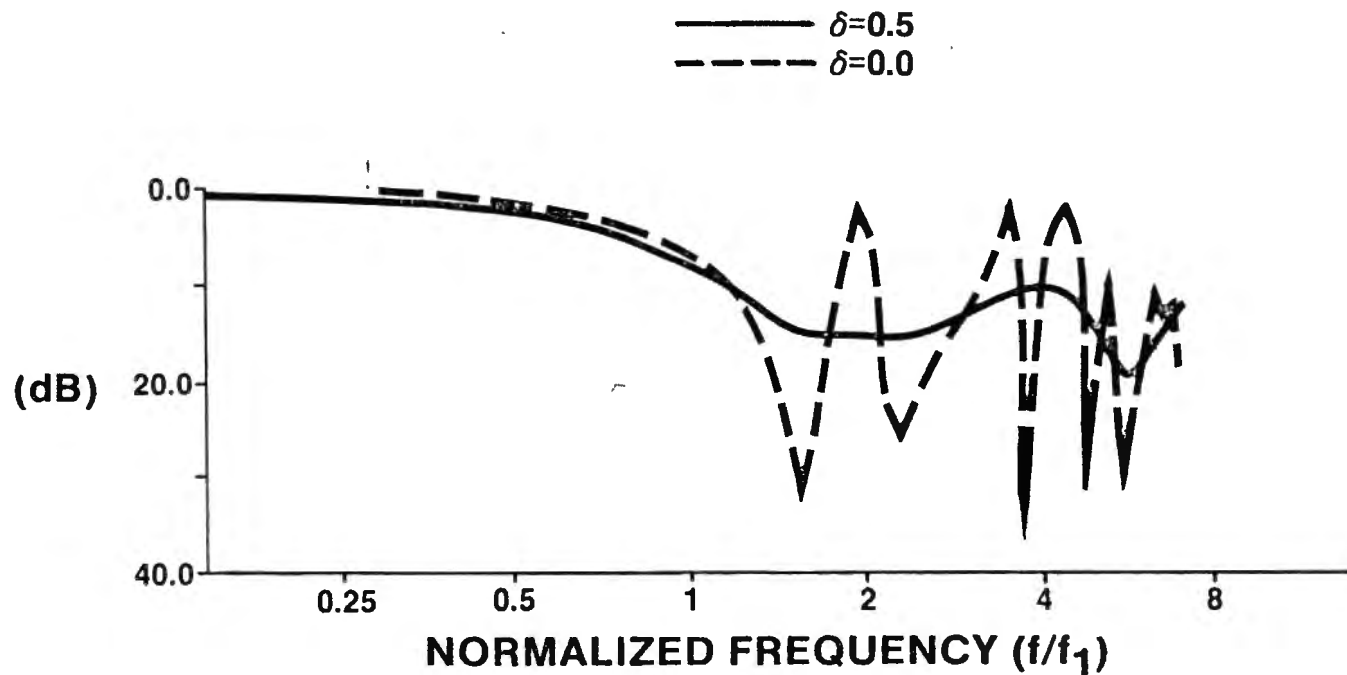
FIGURE 8

CALCULATIONS OF INSERTION LOSS WITH VARIATION OF LAYER THICKNESS (t)

HIGH SHEAR ($\mu=10^8$ N/m^2 $\delta=0.5$)

FIGURE 9
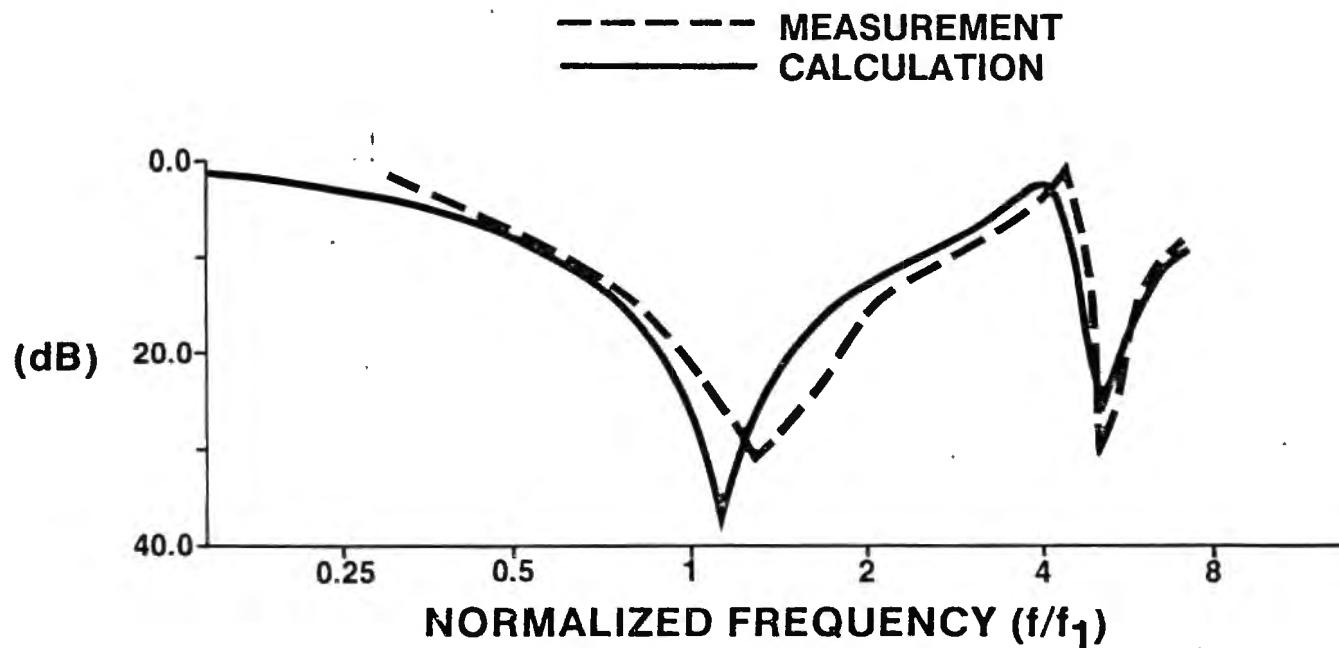
L3818iS

CALCULATED AND MEASURED INSERTION
LOSS FOR A LOW SHEAR MATERIAL
$\mu = 10^6$ N/m^2
$\delta = 0.2$
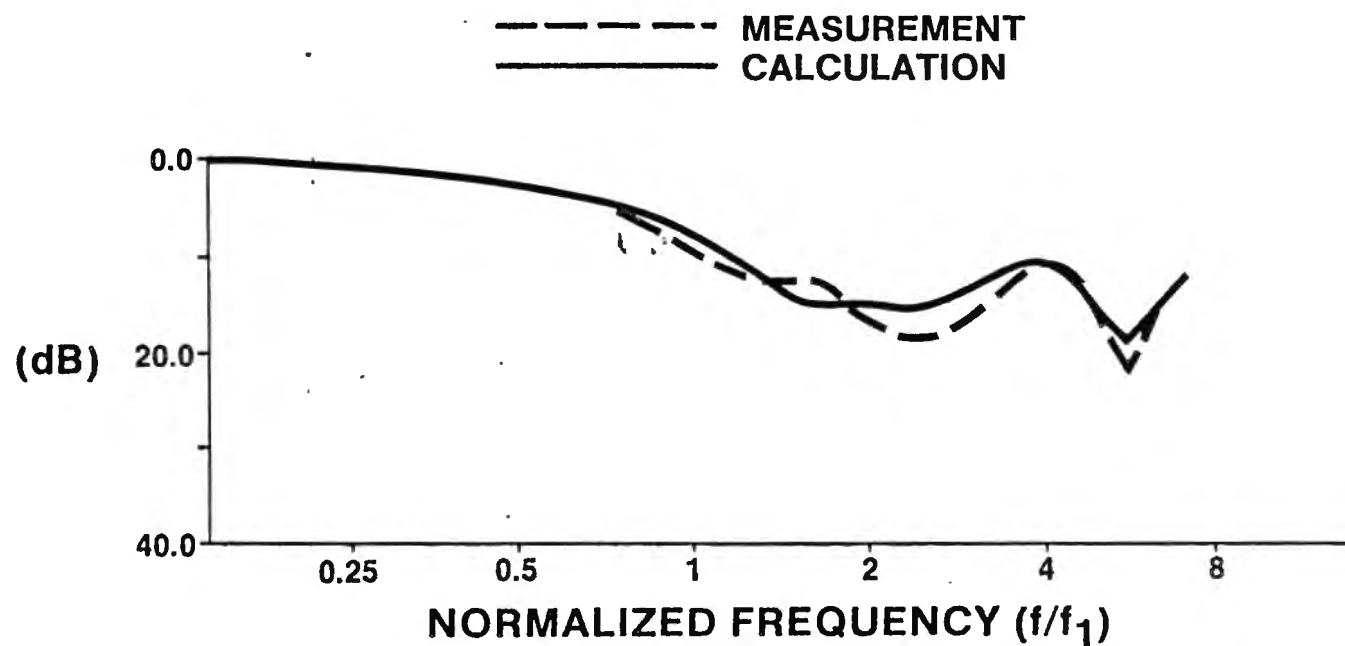
FIGURE 10

L3818kS

CALCULATED AND MEASURED INSERTION
LOSS FOR A HIGH SHEAR MATERIAL
$\mu = 10^8$ N/m^2
$\delta = 0.5$

FIGURE 11

Copy to:

NAVSEA 63R (C. C. Walker)
      55N (C. C. Taylor)
DTNSRDC Code 1905.2 (Dr. W. T. Reader)
       Code 1965 (Dr. Melvin Rummerman, Jerome Goodman)
       Code 1908 (R. A. Rippeon)
Honeywell, Inc. Marine Science Division, (Dr. Murray Simon)
Cambridge Collaboative (Dr. James A. Moore)
NAVSURFWPNCEN (Dr. G. C. Gaunard, Dr. W. Madigowsky)
Bolt, Beranek, Newman/San Diego (Joel Young)

Internal Distribution:
00
01
01A
10
101, Dr. E. Sullivan
322
323 (J. J. Libuha, Dr. W. Strawderman)
3233 (Dr. H. H. Schlomer)
3233 (E. Recine, R. Gay, R. Christman, R. Maple)
3234 (Dr. S. Ko, D. T. Porter, J. Lindberg, G. Battista)
3292 (Dr. C. H. Sherman)
33
332
3321
3321 (F. P. Fessenden, R. C. Turner, L. Carlton, R. Janus)
3322
3323
3323 (D. Power)
3634 (Dr. B. Sandman)
44 (A. Carlson)
721
7212 (3)
7223
72245